New Prognostic Index to Detect the Severity of Asthma Automatically Using Signal Processing Techniques of Capnogram

Mohsen Kazemi[(1)] - Aik Howe Teo[(2)]

(1) Assistant Professor – Department of Electrical Engineering, Khomeinishahr Branch, Islamic Azad University, Khomeinishahr, Isfahan, Iran

(2) Associate Professor - Emergency Department, Hospital Pulau Penang, Malaysia

Abstract

In this paper, a new prognostic index to detect the severity of asthma by processing capnogram signals is presented. Previous studies have shown significant correlation between the capnogram and asthmatic patient. However, most of them used conventional time-domain methods and based on assumption that the capnogram is a stationary signal. In this study, by using linear predictive coding (LPC) coefficients and autoregressive (AR) modelling (Burg method), the capnogram signals are processed. Then, a number of six features including $\alpha 1$, and $\alpha 4$ from LPC and power spectral density (PSD) parameters through AR modelling are extracted. After that, by means of receiver operating characteristic (ROC) curve, the effectiveness of the extracted features to differentiate between asthmatic and nonasthmatic conditions is justified. Finally, selected features are used in a Gaussian radial basis function (GRBF) network. The output of this network is an integer prognostic index ranging from 1 to 10 (depends on the severity of asthma) with an average good detection rate of 90.15% and an error rate of 9.85%. In the other word, based on the results, sensitivity and specificity of this algorithm are 93.54% and 98.29%, respectively. This developed algorithm is purposed to provide a fast and low-cost diagnostic system to help healthcare professional involved in respiratory care as it would be possible to monitor severity of asthma automatically and instantaneously.

Index Terms: Asthma, Autoregressive modelling, Capnogram, Linear predictive coding, Radial basis function neural network

1. Introduction

Asthma is a chronic inflammatory disease of the bronchial tubes that occurs in about 5% of all people and continues to be a significant cause of morbidity and mortality [1]. Traditionally, peak flow meter and spirometer is used to monitor the asthmatic patients which have lots of limitations [2]. Nowadays, capnography is a new method used to monitor the asthmatic conditions. Unlike traditional methods, it is taken while the patient is breathing as comfortable as possible without requiring any complicated instructions [3].

Capnography uses the technology of infrared to determine the concentration of carbon dioxide. Capnogram is the graphical display of instantaneous CO_2 concentration (mmHg) versus time (second). It is able to show changes in gas exchange of the patients. A normal capnogram has four phases and an end-tidal point, as shown in Fig. (1). Each phase reflects the process of CO_2 elimination. The flat phase *I* describes early exhalation and as inhalation occurs, a near-vertical rapidly falling phase *IV* is observed.

In normal ventilation and perfusion, $PetCO_2$ should read 2-5 mmHg higher than the $PACO_2$ [4]. Nevertheless, a wide range of airway disease can lead to incomplete alveolar emptying [5].
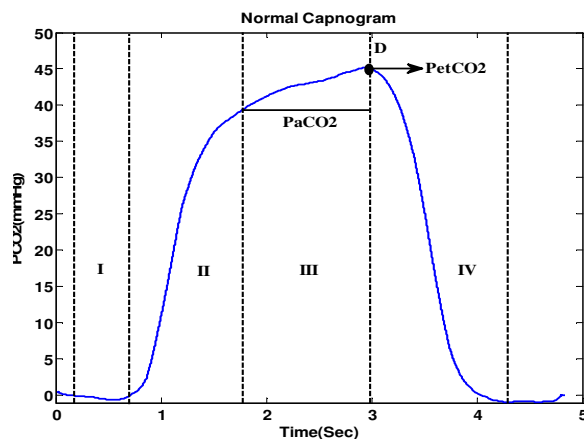
Fig. (1): A normal capnogram

Therefore, the true end tidal point was never reached. Fig.2 (b) shows the capnogram of an asthmatic patient with an obstruction in some parts of the breathing circuit. It should be considered that the ascending limb of the capnogram is prolonged and is not flat, as it should be normally as shown in Fig.2 (a). These changes give rise to the so called "shark's fin" morphology capnogram in patients with airway obstruction. However, it could be found more abnormal capnogram that depending on the patient's condition [6].

Corresponding Author: Mohsen Kazemi, Department of Electrical Engineering, Khomeinishahr Branch, Islamic Azad University, Khomeinishahr, Isfahan, Iran, mohsenkazemi20@gmail.com
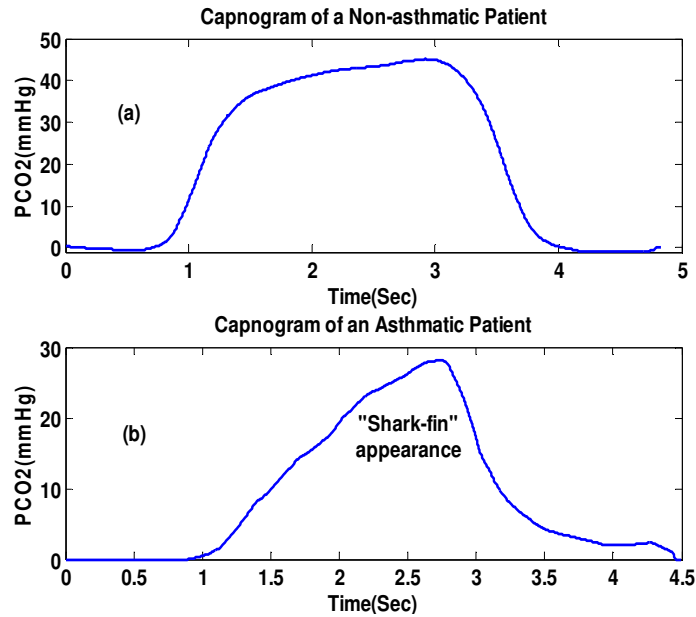
Fig. (2): Comparing waveforms: (a) Normal capnogram and (b) Asthmatic capnogram

These variations in capnogram of different diseases cause the researchers carry out analysis of this signal to differentiate between a range of airway illnesses; especially for asthmatic and nonasthmatic conditions [7-10]. However, all these previous studies are conducted through time domain techniques and based on assumption that capnogram is a stationary signal. But, according to the new findings, capnogram is a wide-sense nonstationary signal [11] which means time-varying information is important. In this research, features of capnogram are extracted to characterize the severity of asthma in patients. The linear predictive coding (LPC) coefficients are proposed to use because these parameters are suitable for capnogram which has slope changes for a lot of airway abnormalities. Furthermore, in frequency domain, the power spectral density (PSD) of the capnogram signals is estimated by using the Autoregressive (AR) modeling as a nonstationary approach. This then has led to differentiation in frequency content of capnogram signal in asthmatic and nonasthmatic conditions. It is important to note that, till today, no study has been performed to analysis capnogram in frequency domain.

Also, selected features are used as an input vector of a Gaussian radial basis function (GRBF) network that is designed to automatically cluster and classify the patients with different asthmatic severity.

In this paper, section 2 discusses the methods proposed which consists of data acquisition, preprocessing, LPC analysis, AR modeling of capnogram signals, performance measure, and RBF neural networks. It is continued with results and discussion at section 3. Lastly, the performance evaluation and the conclusion are presented in section 4 and 5, respectively. So, this study purposes an algorithm to detect severity of asthma based on signal processing techniques of capnogram signal, and GRBF network.

2. Methods

This section contains 6 sub-sections which are presented accordingly. Fig. (3) shows the block diagram of overall steps involved in the proposed algorithm.

The first step is data collection, followed by the preprocessing of capnogram signals. Then, the features of capnogram signal are extracted using LPC analysis and AR modeling in subsections *3* and *4*. It should be noted that the effectiveness of the extracted features is validated by using receiver operating characteristic (ROC) curve analysis and two indices included sensitivity and specificity that are often employed in medical applications [12-14]. Lastly, selected features are used to design a GRBF network to produce a new prognostic index to detect the severity of asthma that is presented in subsection *5*. As it has been discussed in section 3, applying theses methods on capnogram signals result in developing an algorithm to detect severity of asthma in patients who suffer from this acute disease.
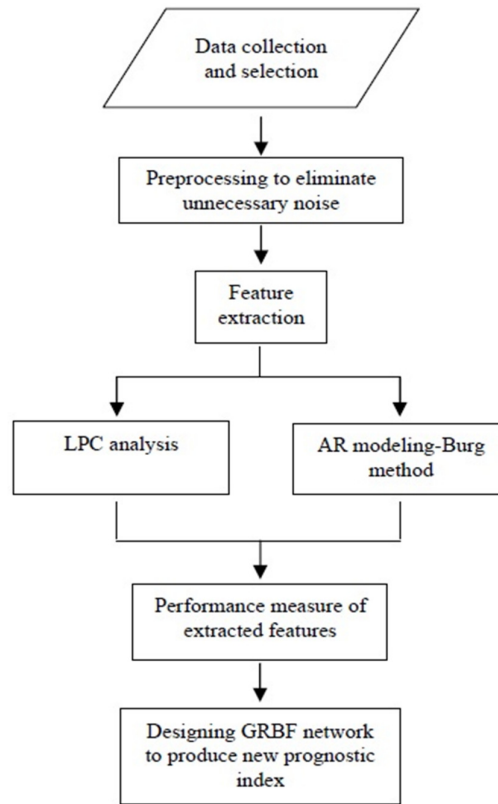
Fig. (3): The overall view of the applied methods

2.1. Data Acquisition

The capnogram data were collected from patients with complaints of asthma and breathing difficulties at the Emergency Department of Hospital Pulau Pinang. Also, non-asthmatic patients have been chosen based on their respiratory disease history and respiratory specialist consultation. Also, All subjects were non-smoker ones and data has been taken while the subject was in sitting position. Informed written consent was obtained from the patients under permission of National Medical Research Section of Ministry of Health Malaysia (MOH) that was approved by the ethics committee of Hospital Pulau Pinang.

Fig. (4) shows the block diagram of data collection in brief. From this figure, as the first step to collect data, the capnography sensor was attached on the mouth or nose of the patients. Side-stream capnography method was used in the process of data collection because this method has higher accuracy [15]. After attaching the sensor on the patient's nose or mouth, the continuous capnogram was recorded using the capnography patient monitor, Capnostream^{TM}20 Model CS08798. Then, the capnogram data was transferred to a personal computer for analysis. Throughout the study, a total of 23 nonasthmatic capnogram, and 73 asthmatic capnogram were successfully collected from 96 persons. The capnogram for each patient was recorded around five minutes at a sampling frequency of 20Hz. Then, a continuous and complete part of recorded data with the length of five breathing cycles and without any artifact (approximately 20 seconds; according to the patient's respiratory rate) was extracted for further analysis.

It should be noted that severity of asthma in patients has been assessed using PEFR (Peak expiratory flow rate), FEV1 (Forced expiratory volume in 1 second) and clinical judgment (in some subjects that obtaining first two indices were difficult due to emergency situations) by the physician and his specialist team in the Hospital. Besides, these tests have been made in different stages of the acute asthmatic attack, i.e. early full symptomatic phases, mid-treatment phase after some initial nebulisation, and end-treatment phase when the patient is symptomatically better and clinically available for discharge home.
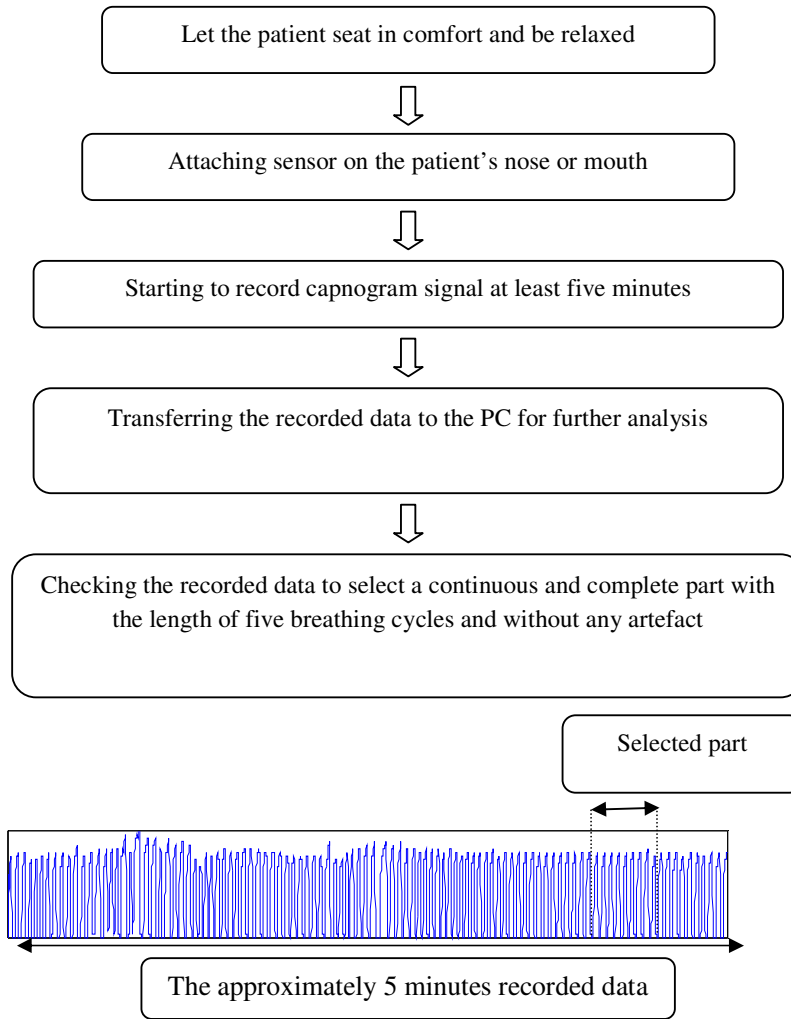
Fig. (4): The block diagram of data collection in brief

2.2 Preprocessing

Data preprocessing was carried out to eliminate unnecessary noise in the recorded capnogram signals. In this paper, the moving average filtering method was used to smooth the curve due to its simplicity and efficiency, especially for eliminating the high frequency noises within the signals [16]. This method smoothes data by replacing each data point with the average of neighboring data points defined within a specific span. This process is equivalent to lowpass filtering with the response of the smoothing given by the difference equation as follow:

$$y_s = \left(y(i+N) + y(i+N-1) + ... + y(i-N) \right)/(2N+1) \quad (1)$$

where $y_s(i)$ is the smoothed value for the *ith* data point, N is the number of neighboring data points on either side of $y_s(i)$, and *2N+1* is the span. Indeed, the span defines a window that moves across the data set as the smoothed response value is calculated for each predictor value. A large span increases the smoothness but decreases the resolution of the smoothed data set, while a small span decreases the smoothness but increases the resolution of the smoothed data set [17]. The optimal span value depends on the data set and usually requires some trial and error to determine [18]. In this study, we used the span as 13, because it produced the best results for both smoothness and resolution. Furthermore, the correlation coefficients calculated for each signal after filtering justified this span width. Fig.5 shows the correlation coefficients for some of capnogram signals after filtering with use of different spans. This figure shows the similarity of signal with itself after and before filtering, and shows that with selecting the span as 13, this similarity is maximum value and is near 1, that approves selecting 13 for span is a good choice. It should be noted that this correlation coefficient for all signals, before and after filtering, has been calculated and the results were same, but only some of them are presented in this figure.

56
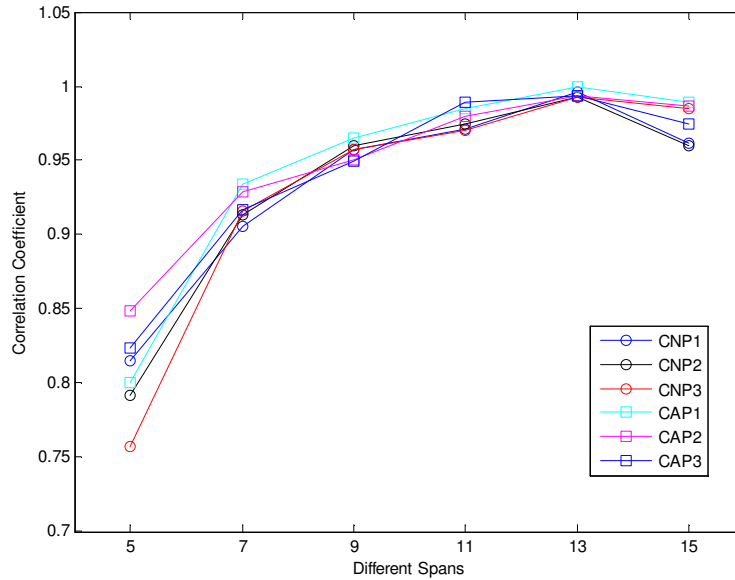
Fig. (5): The correlation coefficients of some capnogram signals after filtering with different spans

2.3 LPC Analysis

LPC is a method to model the signal source through observation of input and output sample sequences. The basic concept of LPC analysis is to estimate a functional set of component coefficients which represent the behavior of a system where each expression sample is approximated as a combination of past samples [19], i.e. for a signal sample $x(n)$ is:

$$x(n) = \sum_{k=1}^{p} \alpha_k x(n-k) \qquad (2)$$

where α_k and p are LPC coefficients and order, respectively.

The aim of the LPC analysis is estimating the best prediction coefficients α_k through the number of n data samples and put the order p of the required predictor (normally $n>>p$), so that the predicted expression sample is the best approximation of the original expression sample [20]. The least-squares minimization method based on minimizing the mean energy in the expression variation over n expression samples of the dataset is used to calculate the predictor coefficients. This process leads to a system of p equations with p unknowns which should be solved to find the best fitting predictor coefficients [21].

There are a number of approaches to solve these linear equations. The most common one is the covariance method which is the efficient linear prediction for spectral estimation techniques and is appropriate to estimate coefficients from a sample of a nonstationary signal [22].

2.4. AR Modelling

Autoregressive (AR) models are widely used for power spectral density (PSD) estimation [23]. The AR model of a time series is represented in the

following form:

$$x(n) = -\sum_{m=1}^{P} a(m)x(n-m) + e(n) \qquad (3)$$

where $x(n)$ is the time series, $a(m)$ are AR parameters, P is the model order, and $e(n)$ is the prediction error.

A variety of AR models are currently used to estimate the PSD of biomedical signals. The Burg method was selected because, as shown in equations (5) and (6), it estimates the reflection coefficients, but other methods such as autocorrelation approach, use prediction coefficients for the AR process. So, in comparison with other approaches such as autocorrelation, covariance, modified covariance, and recursive least squares (RLS), this method does not require run-off of the data sequence by zero padding and has minimal phase characteristic with high accuracy [24].

The minimization criteria of the Burg method are obtained by minimizing the sum-squared of the forward and backward prediction errors as follows:

$$\varepsilon = \sum_{n=P}^{N-1} \left[e_p^f(n)^2 + e_p^b(n)^2 \right] = \min \qquad (4)$$

where $e_p^f(n)$ is the forward prediction error at the pth stage, $e_p^b(n)$ is the backward prediction error at the pth stage, N is the total number of data points, and P represents the model order.

Burg minimized the performance index with respect to the reflection coefficients as follows:

$$\frac{\partial \varepsilon}{\partial \gamma_p} = 2 \sum_{n=P}^{N-1} \left[e_p^f(n) \frac{e_p^f(n)}{\partial \gamma_p} + e_p^b(n) \frac{e_p^b(n)}{\partial \gamma_p} \right] = 0 \qquad (5)$$

where γ_p are the reflection coefficients. Then, the forward and backward prediction errors can be calculated by using lattice filters, and as a result the reflection coefficients γ_p can be obtained as follow:

$$\gamma_p = \frac{2\sum_{n=P}^{N-1} e_{p-1}^f(n)e_{p-1}^b(n-1)}{\sum_{n=P}^{N-1}\left[e_{p-1}^f(n)^2 + e_{p-1}^b(n-1)^2\right]} \tag{6}$$

One of the crucial parts for the AR method is the selection of appropriate value for the model order P. In spectral estimation, the accuracy of the estimated spectrum is critically dependent on the model order that is chosen. It means that a too low model order can generate an over smoothed spectrum, whereas too high a value of order may introduce spurious details such as false peaks into spectrum [25].

The model order can be estimated using the Akaike information criterion (AIC) which is one of the popular methods to establish an optimum model order and minimize the information entropy of the signal identified as follows [26]:

$$AIC(p) = N\ln(E_p) + 2P \tag{7}$$

where E_P, P, and N individually represent the estimation of mean-squared error, the order of the filter, and the number of input signal samples.

In this study, the AIC for different model orders were calculated. Based on the results, at $P=10$ the AIC value (-4.4) was smallest compared to the other number of P. So, the model order 10 was selected since the minimum of error variance was observed at this value of P.

2.5. GRBF Neural Networks

A radial basis network is a feed-forward neural network using the radial basis activation function. An RBF network generally consists of two weight layers; the hidden layer and the output layer, which can be described as follows [27]:

$$y = w_0 + \sum_{i=1}^{n_h} w_i f\left(\|X - c_i\|\right) \tag{8}$$

where f are the radial basis functions, w_i are the output layer weights, w_0 is the output offset, X are inputs to the network, c_i are the centers associated with the basis functions, and n_h is the number of basis functions in the network. Furthermore, the $\| . \|$ denotes the Euclidean norm that measures the size of the vector in a general sense and is defined as:

$$\|X\| = \left(\sum_{i=1}^{n} x_i^2\right)^{1/2} = (X'X)^{1/2}, X = [x_1,..., x_n]' \tag{9}$$

The nonlinear basis function, f, can be formed using a number of different functions that the most common choice is the Gaussian function [28]. The GRBF network can be written using conventional time series notation as:

$$y(t) = Z'(t)W \tag{10}$$

where W is the output layer weight vector and $Z(t)$ is the basis function output vector at time t given, respectively, by:

$$W = [w_0, w_1,...,w_{n_h}]'$$

$$Z = [1, z_1(t),...z_{n_h}(t)]'$$

$$z_i(t) = \exp\left(-\|X(t) - c_i\|^2 / r_i^2\right), X(t) = [x_1(t),...,x_{n_h}(t)]' \tag{11}$$

where c_i and r_i are ith basis function centre vector and ith basis function width, respectively, and $X(t)$ is input vector.

3 Results and Discussion

In this section, the results of LPC analysis, the estimated PSD using AR modeling-Burg method, and the new prognostic index produced by using GRBF network are thoroughly presented and discussed in section 3.1, 3.2 and 3.3 accordingly.

3.1 LPC Analysis Results

For this analysis, we use LPC with order 8 ($p = 8$) because capnogram is related to breath. The average respiratory rate reported in a healthy adult at rest is usually given as 12 breaths per minute, but estimates do vary between sources, although according to be healthy, unhealthy, and age it could change. However totally it is between 12 to 50 breaths per minute [29], therefore, it has low frequency range, and using LPC with order 8 is suitable. Fig.6 shows the correlation coefficients between the original signal and estimated signals using different LPC orders.

As it can observed from this figure, LPC with order 8 has best correlation coefficient rather than other orders, so this order was chosen for this analysis.

Table 1 shows the sensitivity, specificity, AUC, and P-Value for LPC coefficients. In general, for almost all coefficients, sensitivity and specificity is good.
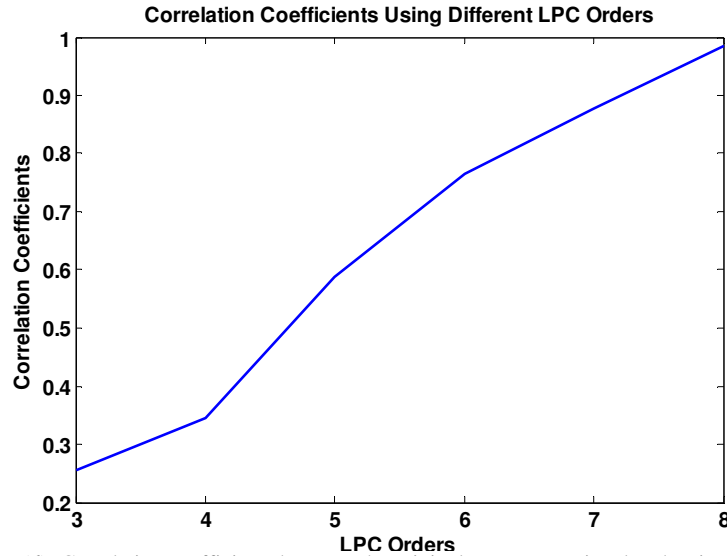
Fig. (6): Correlation coefficients between the original capnogram signal and estimated signals using different LPC orders

Table (1): The performance indices for extracted LPC coefficients

LPC Coefficients	Sensitivity	Specificity	AUC	p-value
α_1	93.55	94.74	0.706	0.0073
α_2	74.19	78.95	0.601	0.214
α_3	70.97	73.68	0.545	0.5899
α_4	96.77	95.63	0.723	0.0019
α_5	87.1	84.21	0.657	0.0762
α_6	71.87	63.16	0.615	0.209
α_7	68.42	51.61	0.557	0.536
α_8	83.87	80.91	0.637	0.0933

Although, α_1, and α_4 have the highest sensitivity (93.55, and 96.77, respectively) and specificity (94.74, and 95.63, respectively) that could be concluded these two coefficients can accurately differentiate asthmatic and non-asthmatic patients. Moreover, all coefficients have AUC > 0.6 and p value <0.2. This shows that almost all of them are able to differentiate the asthmatic and the non-asthmatic conditions. However, it can be seen from Table 1 that, α_1, and α_4 have significant AUC and p-value which is efficient to group the capnogram data into two significant groups which are asthmatic and non-asthmatic patients.

3.2 AR Modelling-Burg Method Results
Fig.7 and Fig.8 show the PSD estimation of a nonasthmatic capnogram (CNP2) and an asthmatic capnogram (CAP9) by using Burg method of AR modeling.
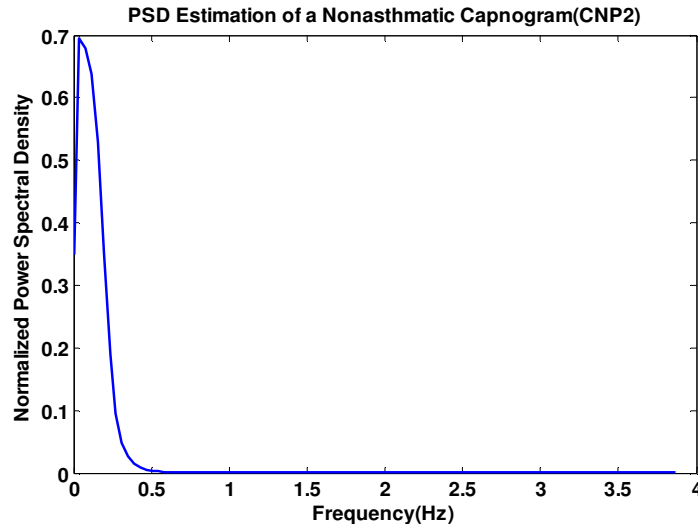
Fig. (7): Power spectral density of a nonasthmatic capnogram (CNP2)
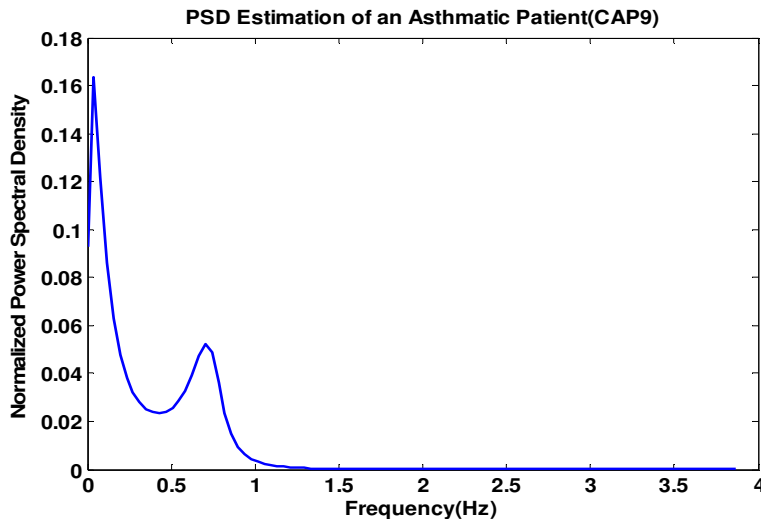
Fig. (8): Power spectral density of an asthmatic capnogram (CAP9)

As shown in Fig.7 and Fig.8, and according to the results for all data, the PSD estimation of the nonasthmatic capnogram signals (CNPs) consists of one component, while for asthmatic capnogram signals (CAPs), this estimation produced two components. Hence by using the second component in PSD estimation using Burg method, asthmatic and nonasthmatic conditions can be differentiated without errors. Also, the mean of frequency of the first component, and the total power of the PSD estimation for asthmatic capnogram were 0.02 Hz (with a standard deviation of 0.006 Hz) and 0.195, respectively, whereas, these values for non-asthmatic capnogram were 0.011 Hz (with a standard deviation of 0.003 Hz) and 0.354, respectively. Table 2 shows performance indices for the frequency of the first component, its magnitude, and the total power in the PSD estimation of the CAPs and CNPs.

Table (2): AUC and p-value for the frequency of the first component and total power in the PSD estimation of CNPs, and CAPs

Performance index	Frequency of the First Component (Hz)	Magnitude of the First Component (Normalized)	Total Power
Sensitivity	98.23	98.3	83.87
Specificity	95.08	93.8	84.21
AUC	0.996	0.97	0.722
p-value	<0.0001	<0.0001	0.0023

According to the Table (2), all features have AUC > 0.7 and p-value < 0.003. This indicated that all parameters in the PSD distribution of CAPs and CNPs are functional in differentiating the asthmatic and nonasthmatic conditions. However, it is obvious that the first component frequency and its magnitude have noticeable AUC and p-value, accompanied by high sensitivity and specificity, which is efficient to classify the capnogram signals in two groups. As a result, these parameters and the frequency of the second component (that only exist in PSD of asthmatic patients) can significantly differentiate the asthmatic severity conditions.

The bottom line is that, the frequency of the second component of the asthmatic capnograms PSD estimation varied in patients with different levels of asthmatic severity. It means that, the average of this value for the very low, low, mild, and serious asthmatic capnograms was 0.18 Hz, 0.25 Hz, 0.43 Hz, and 0.6 Hz, respectively. Also, the standard deviation related to each category was 0.02 Hz, 0.06 Hz, 0.05 Hz, and 0.1 Hz. So, this parameter has been selected as one of the features to carry out this study.

3.3. New Prognostic Index by Using GRBF

Based on the results obtained, our feature vector consists of six elements. These are α_1, and α_4 from LPC analysis, the number of frequency components, magnitude of the first component, and the frequency of the first and second components in PSD estimation by AR modeling-Burg method.

First of all, our database has been divided into two different sets in which one is used for training phase and the other one is used for testing phase. The training set has one additional element in feature vector. This element is the level of severity as indicated by physician who examined our patients. It is represented by a number from one to ten for a nonasthmatic patient to a patient, who suffers from very severe asthma, respectively, that is the main goal of this research.

Before designing the RBF network for the application of the data, as mentioned in previous sections, it needs to be considered that the design of RBF networks consists of two important parts; network construction, and parameter adjustment. Like any other nonlinear network, RBF networks face the same controversy in choosing the number of RBF units. It means that too few RBF units cannot get acceptable approximations, while too many RBF units lead to expensive computation and may cause over-fitting problem [30]. In this research, the process of training was stopped when the number of RBF units was equal to thirty, or the program reached the mean squared error (MSE). This limit for RBF units was selected in order to get the best and most accurate results from the designed GRBF network for this study.

Based on the results, after thirty training epochs, the GRBF network reached the desire MSE. After the training phase, the GRBF network has been loaded with the test datasets. The output of this network is an integer prognostic index ranging from 1 to 10 (depends on the severity of asthma) with an average good detection rate of 90.15% and an error rate of 9.85%. Table (3) shows the detection rate of the RBF network output in more detail.

The bottom line is that, only a total of 6.46% of asthmatic patients' capnogram were detected as non-asthmatic ones and rest of error rates were due to put some asthmatic patients' capnogram in wrong severity level category, e.g. one of the CAPs has been for a patient who suffer from a mild asthma, but is detected as low asthma by the RBF network. So, it can be considered that the sensitivity of our method is 93.54%. Also, it should be noted that an increase in the number of samples to train the RBF network will produce more accurate results (especially for the severe and very severe categories that the RBF network produces poor results since the lack of samples for testing and training phases).

Consequently, the defined index can be used in capnography to detect the severity of asthma in patient with respiratory difficulties with good accuracy and also as an online system.

Table (3): The detection rate of RBF network output in detail

Detection rate index	Asthmatic patients with various severity level					Detection rate index	Non-asthmatic patients
	Very Low	Low	Mild	Severe	Very Severe		
TP (%)	96.66	95.85	94.89	80.25	75	TN (%)	98.29
FN (%)	3.34	4.15	5.11	19.75	25	FP (%)	1.71

4. Performance Evaluation

In this research a new approach to monitor asthmatic patients and to detect the severity of asthma based on signal processing techniques of capnogram is presented. In this section, the performance of our proposed method is compared with two existing algorithms which are "S" parameters [7], and a recently introduced one using Hjorth parameters [10]. First of all, according to the presented algorithms in their researches, the capnogram signals were separated into equal segments to calculate related "S" parameters and Hjorth parameters (for both

whole cycle of capnogram for one breath cycle, and the range of capnogram that is limited between the time at beginning of S1 and time at the end tidal peak) for each cycle. This is the first step to evaluate the performance of these methods on our database.

For this purpose, according to the respiratory rate of each patient, every sample was divided into 5 segments, taking effort that each segment contained

one complete breath cycle. Then, "S" parameters including S1, S2 and SR (based on You et al study results) and Hjorth parameters were calculated for each cycle. Table (4) shows the performance indices of these methods.

Table (4): The performance indices of presented method in this research in comparison with two existing algorithms

Performance Indices	'S' Parameters Method	Hjorth Parameters Method	Presented Algorithm in This Thesis
Sensitivity (%)	71.32	88.2	93.54
Specificity (%)	72.75	81.74	98.29

As can be seen in Table 4, our presented method has better sensitivity and specificity (93.54% and 98.29%, respectively) in comparison with the two existing approaches. Also, the Hjorth parameters method with 88.2% sensitivity and 81.47% specificity has better performance than "S" parameters approach that could be mostly due to the former algorithm considers the whole parts of capnogram signal to analyze, but the latter algorithm only calculates some indices and slopes of capnogram signal. It should be noted that the reported values for "S" parameters method in Table 4 is combination of three extracted indices.

The first and foremost difference between this research and the existing algorithms is that in this study, it has been approved that the capnogram signal is in category of the wide-sense non-stationary signals, so more than one cycle of this signal is analyzed whereas both the existing algorithms were based on the non-approved fact that capnogram is a stationary signal and only one cycle of capnogram signal was investigated. So, this hypothesis not only limited them to use some conventional time-domain methods, but also the frequency contents of capnogram were ignored.

Therefore, in this study, non-stationary techniques included LPC and AR modeling are used to process capnogram signals in time-domain and to estimate the power spectral density of capnogram signals, respectively. Furthermore, in contrast with existing methods that their results were aimed at differentiating asthmatic and non-asthmatic conditions, in this study, a new prognostic index is introduced to not only differentiate the asthmatic and non-asthmatic conditions, but also to detect the severity of asthma in patients.

In a nutshell, our results show that the presented

method in this research has better performance in comparison with existing methods in monitoring asthmatic patients and in detecting asthmatic and nonasthmatic patients as well as differentiating asthmatic patients with various levels of severity.

5. Conclusions

Capnogram is a vital representation of the respiratory system. Therefore, the analysis of this physiological signal could lead to the development of computerized methods to differentiate airway disorders, which could benefit both the healthcare professional involved in respiratory care and the patients. Previous studies conducted for capnogram signal analysis used only conventional time domain methods. In this paper, for the first time, frequency contents of capnogram signals have been investigated.

The results showed that by using these properties, asthmatic and nonasthmatic conditions can be differentiated. Also, by the incorporation of a GRBF neural network, the severity of asthma in the patients could be automatically assessed as a new index in capnographs. This method is an innovative idea that could further assist the medical practitioners as it would be possible to monitor severity of asthma automatically and instant-aneously with minimum human errors.

References

[1] M.V. Clark, Asthma: A clinician's guide, Jones & Bartlett Learning LLC, 2011.

[2] A. H. Teo, K. Jaalam, R. Ahmad, C.K. Sheng, N. Hisamuddin, "The use of end-tidal capnography to monitor non-intubated patients presenting with acute exacerbation of asthma in the emergency department", J. Emerg. Med., Vol. 41, No. 6, pp. 581-589, March 2009.

[3] C. Rhoades, F. Thomas, Capnography: Beyond the numbers, Air Med. J., Vol. 21, No. 2, pp. 43-48, 2002.

[4] J. Giner, P. Casan, "Pulse oximetry and capnography in lung function laboratories", Arch. Bronconeumol, Vol. 40, No. 7, pp. 311-314, 2004.

[5] J.E. Thompson, M.B. Jaffe, "Capnography waveforms in the mechanically ventilated patient", Respir. Care J., Vol. 50, No. 1, pp. 100-109, 2005.

[6] B. Smalhout, Z. Kalenda, An atlas of capnography, Second ed., Kerckebosche Zeist Press, 1981.

[7] B. You, R. Peslin, C. Duvivier, V. Dang Vu, J. P. Grilliat, "Expiratory capnography in asthma", European Respir. J., Vol. 7, pp. 318-323, 1994.

[8] M. Yaron, P. Padyk, M. Hutsinpiller, C.B. Cairns, "Utility of the expiratory capnogram in the assessment of bronchospasm", Ann. Emerg. Med., Vol. 28, No. 4, pp. 403-407, 1996.

[9] J. Druck, P. M. Rubio, M. A. Valley, M. B. Jaffe, M. Yaron, "Evaluation of the slope of phase III from the volumetric capnogram as a non-effort dependent in acute asthma exacerbation", Ann. Emerg. Med.m Vol. 50, No. 3, pp. 130-136, 2007.

[10] M. Kazemi, N.I. Imarah, M.B. Malarvili, "Assessment on methods used to detect asthmatic and non-asthmatic conditions using capnogram signal", Journal Teknologi (Sciences & Engineering), Vol. 62, No. 1, pp. 93-100, 2013.

[11] M. Kazemi, M.B. Malarvili, "Investigation of capnogram signal characteristics using statistical methods", Proceeding of the IEEE/ IECBES, Langkawi, Malaysia, pp. 343-348, 2012.

[12] A. Temko, G. Lightbody, E.M. Thomas, G.B. Boyland, W. Marnane, "Instantaneous measure of EEG channel importance for improved patient-adaptive neonatal seizure detection", IEEE Trans. on Biomedical Engineering, Vol. 59, No. 3, pp. 717-727, March 2012.

[13] M.M. Fraz, P. Remagnino, A. Hoppe, B. Uyyanonvara, A.R. Rudnicka, C.G. Owen, S.A. Barman, "Blood vessel segmentation methodologies in retinal imagies – A survey", J. Comput. Meth. Prog. Bio., Vol. 108, No. 1, pp. 407-433, 2012.

[14] J.L.M. Amaral, A.J. Lopes, J.M. Jansen, A.C.D. Faria, P.L. Melo, "An improved method of early diagnosis of smoking-induced respiratory changes using machine learning algorithms", J. Comput. Meth. Prog. Bio., Vol. 112, No. 3, pp. 441-454, 2013.

[15] J. Swenson, P.N. Henao-Guerrero, J.W. Carpenter, "Clinical technique: use of capnography in small mammal anesthesia", J. Exot. Pet. Med., Vol. 17, No. 3, pp. 175-180, 2008.

[16] M. Kirkko-Jaakkola, J. Collin, J. Takala, "Bias prediction for MEMS gyroscopes", IEEE Sensors Journal, Vol. 12, No. 6, pp. 2157-2163, June 2012.

[17] A. Facchinetti, G. Sparacino, C. Cobelli, "An online self-tunable method to denoise CGM sensor data", IEEE Trans. on Biomedical Engineering, Vol. 57, No. 3, pp. 634-641, March 2010.

[18] G.R Arce, "Nonlinear signal processing", A Statistical Approach. John Wiley & Sons Inc., New Jersey, 2005.

[19] R. Zamir, Y. Kochman, U. Erez, "Achieving the Gaussian rate-distortion function by prediction", IEEE Trans. on Information Theory, Vol. 54, No. 7, pp. 3354-3364, July 2008.

[20] E. Carotti, J.C. Martin, R. Merletti, D. Farina, "Compression of multidimensional biomedical signals with spatial and temporal codebook-excited linear prediction", IEEE Trans. on Biomedical Engineering, Vol. 56, No. 11, pp. 2604-2610, Nov. 2009.

[21] G. Kannan, A.A. Milani, I. Panahi, R. Briggs, "An efficient feedback active noise control algorithm based on reduced-order linear predictive modeling of fMRI acoustic noise", IEEE Trans. on Biomedical Engineering, Vol. 58, No. 12, pp. 3303-3309, Dec. 2011.

[22] R. Istepanian, A. Sungoor, J.C. Nebel, "Comparative analysis of genomic signal processing for microarray data clustering", IEEE Trans. on NanoBioscience, Vol. 10, No. 4, pp. 225-238, Dec. 2011.

[23] H.W. Hsu, C.M. Liu, "Autoregressive modeling of temporal/spectral envelopes with finite-length discrete trigonometric transforms", IEEE Trans. on Signal Processing, Vol. 58, No. 7, pp. 3692-3705, July 2010.

[24] K.J. Blinowska, J. Zygierewicz, "Practical biomedical signal analysis", CRC Press (Taylor & Francis Group, LLC), Poland, 2011.

[25] T. Cassar, K.P. Camilleri, S.G. Fabri, "Order estimation of multivariate ARMA models", IEEE Journal of Selected Topics in Signal Processing, Vol. 4, No. 3, pp. 494-503, April 2010.

[26] F.X. Wu, W.J. Zhang, "Dynamic-model-based method for selecting significantly expressed genes from time-course expression profiles", IEEE Trans. on Information Technology in Biomedicine, Vol. 14, No. 1, pp. 16-22, 2010.

[27] T.Y. Lee, S.A. Chen, H.Y. Hung, Y.Y. Ou, "Incorporating distant sequence features and radial basis function networks to identify ubiquitin conjugation sites", PLOS ONE, Vol. 6, No. 3, 2011.

[28] H.X. Huan, D.T.T. Hien, H.H. Tue, "Efficient algorithm for training interpolation RBF networks with equally spaced nodes", IEEE Trans. on Neural Networks, Vol. 22, No. 6, pp. 982-988, 2011.

[29] Lauralee Sherwood, Fundamentals of Physiology: A Human Perspective. Thomson Brooks and Cole Inc, 2006.

[30] B.M. Wilamowski, H. Yu, "Neural network learning without back-propagation", IEEE Trans. on Neural Networks, Vol. 21, No. 11, pp. 1793-1803, 2010.